*ACTA ASTRONOMICA*
Vol. **56** (2006) pp. 307–332

# Binary Lenses in OGLE-III EWS Database. Season 2004

by

M. Jaroszyński, J. Skowron, A. Udalski, M. Kubiak,
M.K. Szymański, G. Pietrzyński, I. Soszyński,
K. Żebruń, O. Szewczyk and Ł. Wyrzykowski

Warsaw University Observatory, Al. Ujazdowskie 4, 00-478 Warszawa, Poland
e-mail:(mj,jskowron,udalski,mk,msz,pietrzyn,soszynsk,zebrun,szewczyk,wyrzykow)
@astrouw.edu.pl

*Received December 18, 2006*

ABSTRACT

We present 19 binary lens candidates from OGLE-III Early Warning System database for the season of 2004. We have also found five events interpreted as single mass lensing of double sources. The candidates have been selected by visual light curves inspection. Examining the models of binary lenses of this and our previous studies (10 caustic crossing events of OGLE-II seasons 1997–1999 and 15 binary lens events of OGLE-III seasons 2002–2003) we find one case of extreme mass ratio binary ($q \approx 0.005$, a known planetary lens OGLE 2003-BLG-235/MOA 2003-BLG-53) and almost all other models with mass ratios in the range $0.1 < q < 1.0$, which may indicate the division between planetary systems and binary stars.

**Key words:** *Gravitational lensing – Galaxy: center – binaries: general*

## 1. Introduction

In this paper we present the results of the search for binary lens events among microlensing phenomena discovered by the Early Warning System (EWS – Udalski *et al.* 1994, Udalski 2003) of the third phase of the Optical Gravitational Lensing Experiment (OGLE-III) in the season of 2004. This is a continuation of the study of binary lenses in OGLE-II (Jaroszyński 2002, hereafter Paper I) and OGLE-III databases (Jaroszyński *et al.* 2004, hereafter Paper II). The results of the similar search for binary lens events in MACHO data have been presented by Alcock *et al.* (2000).

The motivation of the study remains the same – we are going to obtain a uniform sample of binary lens events, selected and modeled with the same methods for all seasons. The sample may be used to study the population of binary systems

in the Galaxy. The method of observation of the binaries (gravitational lensing) allows to study their mass ratios distribution, since they are directly given by the models. The binary separations are more difficult, because only their projection into the sky expressed in Einstein radius units enters the models. In small number of cases the estimation of the masses and distances to the lenses may be possible.

Cases of extremely low binary mass ratios ($q \leq 0.01$) are usually considered as planetary lensing. Such events have been discovered in OGLE-III database for season 2003 (Bond *et al.* 2004) and 2005 (Udalski *et al.* 2005, Gould *et al.* 2006, Beaulieu *et al.* 2006), but are missing in season 2004.

Our approach follows that of Papers I and II, where the references to earlier work on the subject are given. Some basic ideas for binary lens analysis can be found in the review article by Paczyński (1996).

Paper I presents the analysis of 18 binary lens events found in OGLE-II data with 10 safe caustic crossing cases. Paper II gives 15 binary lens events.

In Section 2 we describe the selection of binary lens candidates. In Section 3 we describe the procedure of fitting models to the data. The results are described in Section 4, and the discussion follows in Section 5. The extensive graphical material is shown in Appendix.

## 2. Choice of Candidates

The OGLE-III data is routinely reduced with difference photometry (DIA, Alard and Lupton 1998, Alard 2000) which gives high quality light curves of variable objects. The EWS system of OGLE-III (Udalski 2003) automatically picks up candidate objects with microlensing-like variability.

There are 608 microlensing event candidates selected by EWS in the 2004 season. We visually inspect all candidate light curves looking for features characteristic for binary lenses (multiple peaks, U-shapes, asymmetry). Light curves showing excessive noise are omitted. We select 25 candidate binary events in 2004 data for further study. For these candidate events we apply our standard procedure of finding binary lens models (compare Papers I, II and Section 3).

## 3. Fitting Binary Lens Models

The models of the two point mass lens were investigated by many authors (Schneider and Weiss 1986, Mao and DiStefano 1995, DiStefano and Mao 1996, Dominik 1998, to mention only a few). The effective methods applicable for extended sources have recently been described by Mao and Loeb (2001). While we use mostly the point source approximation, we extensively employ their efficient numerical schemes for calculating the binary lens caustic structure and source magnification.

We fit binary lens models using the $\chi^2$ minimization method for the light curves. It is convenient to model the flux at the time $t_i$ as:

$$F_i = F(t_i) = A(t_i) \times F_s + F_b \equiv (A(t_i) - 1) \times F_s + F_0 \tag{1}$$

where $F_s$ is the flux of the source being lensed, $F_b$ the blended flux (from the source close neighbors and possibly the lens), and the combination $F_b + F_s = F_0$ is the total flux, measured long before or long after the event. The last parameter can be reasonably well estimated with observations performed in seasons preceding and following 2004, as a weighted mean:

$$F_0 = \frac{\sum\limits_{i'=1}^{N'} \frac{F_i}{\sigma_i}}{\sum\limits_{i'=1}^{N'} \frac{1}{\sigma_i}} \tag{2}$$

where $F_i$ are the observed fluxes and $\sigma_i$ their estimated photometric errors. The summation over $i'$ does not include observations of 2004, and $N'$ is the number of relevant observations.

In fitting the models we use rescaled errors (compare Papers I and II). More detailed analysis (*e.g.*, Wyrzykowski 2005) shows that the OGLE photometric errors are overestimated for very faint sources and underestimated for bright ones. Error scaling used here, based on the scatter of the source flux in seasons when it is supposedly invariable, is the simplest approach. It gives the estimate of the combined effect of the observational errors and possibly undetectable, low amplitude internal source variability. We require that constant flux source model fits well the other seasons data after error rescaling:

$$\chi^2_{\rm other} = \sum_{i'=1}^{N'} \frac{(F_i - F_0)^2}{(s\sigma_i)^2} = N' - 1 \tag{3}$$

where $s$ is the error scaling factor.

The lens magnification (amplification) of the source $A(t_i) = A(t_i; p_j)$ depends on the set of model parameters $p_j$. Using this notation one has for the $\chi^2$:

$$\chi^2 = \sum_{i=1}^{N} \frac{((A_i - 1)F_s + F_0 - F_i)^2}{\sigma_i^2}. \tag{4}$$

The dependence of $\chi^2$ on the binary lens parameters $p_j$ is complicated, while the dependence on the source flux is quadratic. The equation $\partial\chi^2/\partial F_s = 0$ can be solved algebraically, giving $F_s = F_s(p_j; \{F_i\})$, thus effectively reducing the dimension of parameter space. Any method of minimizing $\chi^2$ may (in some cases) give unphysical solutions with $F_s > F_0$, which would imply a negative blended flux. To reduce the occurrence of such faulty solutions we add an extra term to $\chi^2$ which

vanishes automatically for physically correct models with $F_s \leq F_0$, but is a fast growing function of the source flux $F_s$ whenever it exceeds the base flux $F_0$.

Our analysis of the models, their fit quality etc. is based on the $\chi^2_1$ calculated with the rescaled errors:

$$\chi^2_1 \equiv \frac{\chi^2}{s^2} \tag{5}$$

which is displayed in the tables and plots below. For events with multiple models (representing different local minima of $\chi^2$), we assess the relevance of each model with the relative weight $w \sim \exp(-\chi^2_1/2)$.

For most of the light curves we investigate the caustic crossings are not well sampled and we are forced to use a point source approximation in majority of our models. In three cases (events OGLE 2004-BLG-035, OGLE 2004-BLG-039, and OGLE 2004-BLG-207) the caustic crossings are resolved, so the extended source models can be fitted. In these cases the strategy resembling Albrow *et al.* (1999) for finding binary lens models can be used. It is based on the fact that some of the parameters (the source angular size, the strength of the caustic) can be fitted independently, so for an initial fit one can split the parameter space into two lower dimensionality sub-manifolds.

The binary system consists of two masses $m_1$ and $m_2$, where by convention $m_1 \leq m_2$. The Einstein radius of the binary lens is defined as:

$$r_{\rm E} = \sqrt{\frac{4G(m_1+m_2)}{c^2}\frac{d_{\rm OL}d_{\rm LS}}{d_{\rm OS}}} \tag{6}$$

where $G$ is the constant of gravity, $c$ is the speed of light, $d_{\rm OL}$ is the observer–lens distance, $d_{\rm LS}$ is the lens–source distance, and $d_{\rm OS} \equiv d_{\rm OL} + d_{\rm LS}$ is the distance between the observer and the source. The Einstein radius serves as a length unit and the Einstein time: $t_{\rm E} = r_{\rm E}/v_\perp$, where $v_\perp$ is the lens velocity relative to the line joining the observer with the source, serves as a time unit. The passage of the source in the lens background is defined by seven parameters: $q \equiv m_1/m_2$ $(0 < q \leq 1)$ – the binary mass ratio, $d$ – binary separation expressed in $r_{\rm E}$ units, $\beta$ – the angle between the source trajectory as projected onto the sky and the projection of the binary axis, $b$ – the impact parameter relative to the binary center of mass, $t_0$ – the time of closest approach of the source to the binary center of mass, $t_{\rm E}$ – the Einstein time, and $r_s$ the source radius. Thus we are left with the seven or six dimensional parameter space, depending on the presence/absence of observations covering the caustic crossings.

We begin with a scan of the parameter space using a logarithmic grid of points in $(q,d)$ plane $(10^{-3} \leq q \leq 1,\ 0.1 \leq d \leq 10)$ and allowing for continuous variation of other parameters. The choice of starting points combines systematic and Monte Carlo searching of regions in parameter space allowing for caustic crossing or cusp approaching events. The $\chi^2$ minimization is based on downhill method and uses standard numerical algorithms. When a local minimum is found we make a

T a b l e 1

The binary lens models of season 2004 events

| year | event | | $\chi^2_1$/DOF | $s$ | $q$ | $d$ | β | $b$ | $t_0$ | $t_E$ | $f$ |
|---|---|---|---|---|---|---|---|---|---|---|---|
| 2004 | 035 | b | 216.0/236 | 2.12 | 0.119 | 1.019 | 57.35 | 0.15 | 3085.7 | 67.3 | 0.78 |
| 2004 | 039 | b | 399.0/382 | 1.94 | 0.094 | 1.165 | 174.39 | −0.11 | 3082.4 | 38.9 | 0.88 |
| 2004 | 207 | b | 501.7/387 | 1.56 | 0.308 | 1.634 | 62.86 | 0.78 | 3151.8 | 28.7 | 0.84 |
| 2004 | 226 | b | 361.3/309 | 1.48 | 0.323 | 1.401 | 296.26 | −0.40 | 3147.7 | 32.9 | 0.67 |
| | | b | 363.9/309 | 1.48 | 0.078 | 0.992 | 161.51 | 0.16 | 3142.0 | 39.5 | 0.25 |
| 2004 | 250 | b | 276.9/274 | 2.04 | 0.705 | 0.830 | 155.04 | −0.12 | 3160.8 | 75.2 | 0.11 |
| 2004 | 273 | b | 241.0/233 | 1.93 | 0.450 | 0.550 | 63.99 | 0.06 | 3157.8 | 30.8 | 1.00 |
| 2004 | 280 | b | 182.2/241 | 2.34 | 0.455 | 2.052 | 139.49 | 0.19 | 3181.0 | 26.3 | 0.51 |
| 2004 | 309 | b | 230.6/296 | 2.35 | 0.346 | 1.293 | 14.86 | −0.08 | 3193.1 | 60.4 | 0.12 |
| 2004 | 325 | b | 351.0/349 | 1.62 | 0.528 | 1.193 | 224.64 | 0.06 | 3180.5 | 57.0 | 0.32 |
| 2004 | 347 | d | 293.7/291 | 1.47 | 0.879 | 3.091 | 220.57 | 0.67 | 3263.9 | 54.6 | 0.60 |
| | | d | 296.4/291 | 1.47 | 0.452 | 0.587 | 122.70 | −0.35 | 3208.8 | 35.0 | 0.93 |
| 2004 | 354 | b | 343.4/335 | 3.64 | 0.681 | 1.869 | 74.34 | 0.85 | 3192.8 | 79.2 | 0.03 |
| 2004 | 362 | b | 399.7/418 | 1.93 | 0.267 | 1.036 | 149.07 | −0.27 | 3195.3 | 126.8 | 0.04 |
| 2004 | 366 | b | 213.9/218 | 1.98 | 0.242 | 0.897 | 39.96 | −0.27 | 3198.7 | 187.0 | 0.05 |
| 2004 | 367 | ? | 1422.0/295 | 1.36 | 0.052 | 0.633 | 97.64 | −0.01 | 3180.8 | 44.7 | 0.20 |
| 2004 | 373 | b | 544.7/550 | 1.52 | 0.708 | 0.955 | 231.36 | −0.09 | 3195.6 | 33.9 | 0.38 |
| 2004 | 379 | b | 432.0/339 | 1.41 | 0.687 | 0.821 | 226.94 | 0.14 | 3196.7 | 30.7 | 0.65 |
| 2004 | 406 | b | 422.7/405 | 1.44 | 0.575 | 0.885 | 214.84 | −0.16 | 3190.0 | 22.7 | 0.23 |
| | | b | 423.1/405 | 1.44 | 0.353 | 2.635 | 233.05 | −1.28 | 3120.5 | 69.5 | 0.12 |
| 2004 | 444 | d | 209.6/240 | 1.98 | 0.675 | 1.282 | 241.57 | −0.19 | 3186.8 | 41.0 | 0.02 |
| 2004 | 451 | b | 295.5/313 | 1.51 | 0.227 | 0.963 | 109.45 | 0.23 | 3224.4 | 35.7 | 0.13 |
| 2004 | 460 | b | 340.2/343 | 1.59 | 0.396 | 1.178 | 350.94 | −0.20 | 3204.1 | 33.0 | 0.18 |
| | | b | 344.8/343 | 1.59 | 0.894 | 1.240 | 17.54 | 0.02 | 3200.4 | 31.3 | 0.21 |
| 2004 | 480 | b | 363.0/342 | 1.63 | 0.163 | 1.370 | 322.43 | −0.15 | 3225.1 | 10.4 | 0.71 |
| | | b | 367.3/342 | 1.63 | 0.038 | 0.797 | 200.47 | −0.11 | 3225.3 | 14.2 | 0.41 |
| 2004 | 490 | d | 289.2/313 | 1.80 | 0.111 | 0.722 | 53.63 | −0.17 | 3223.5 | 17.1 | 0.45 |
| | | d | 291.2/313 | 1.80 | 0.001 | 1.515 | 169.49 | 0.17 | 3223.0 | 18.5 | 0.36 |
| 2004 | 559 | ? | 438.2/199 | 1.78 | 0.658 | 0.881 | 91.86 | 0.06 | 3269.4 | 17.9 | 0.27 |
| 2004 | 572 | b | 259.7/240 | 1.26 | 0.793 | 0.760 | 270.06 | 0.03 | 3288.0 | 31.0 | 0.16 |
| 2004 | 605 | d | 370.8/410 | 1.57 | 0.227 | 0.671 | 19.94 | 0.07 | 3309.9 | 80.6 | 0.16 |
| | | d | 374.9/410 | 1.57 | 0.193 | 3.801 | 77.56 | 2.89 | 3477.3 | 264.8 | 0.12 |

Note: The columns show: the event year and EWS number, the event classification ("b" for a binary lens, "d" for a double source event, "?" for low quality fits and/or uncompelling cases), the rescaled $\chi^2_1$, number of DOF, the scaling factor $s$, the mass ratio $q$, the binary separation $d$, the source trajectory direction β, the impact parameter $b$, the time of the closest center of mass approach $t_0$, the Einstein time $t_E$ and the blending parameter $f \equiv F_s/F_0$.

small Monte Carlo jump in the parameter space and repeat the downhill search. In some cases it allows to find a different local minimum. If it does not work several times, we stop and try next starting point.

Only the events with characteristics of caustic crossing (apparent discontinuities in observed light curves, U-shapes) can be treated as safe binary lens cases. The double peak events may result from cusps approaches, but may also be produced by double sources (*e.g.*, Gaudi and Han 2004). In such cases we also check the double source fit of the event postulating:

$$F(t) = A(u_1(t)) \times F_{s1} + A(u_2(t)) \times F_{s2} + F_b \tag{7}$$

where $F_{s1}$, $F_{s2}$ are the fluxes of the source components, $F_b$ is the blended flux, and $A(u)$ is the single lens amplification (Paczyński 1986). The dimensionless source – lens separations are given as:

$$u_1(t) = \sqrt{{b_1}^2 + \frac{(t-t_{01})^2}{{t_{\rm E}}^2}} \qquad u_2(t) = \sqrt{{b_2}^2 + \frac{(t-t_{02})^2}{{t_{\rm E}}^2}} \tag{8}$$

where $t_{01}$, $t_{02}$ are the closest approach times of the source components, $b_1$, $b_2$ are the respective impact parameters, and $t_{\rm E}$ is the (common) Einstein time.

## 4. Results

Our fitting procedures applied to selected 25 candidate events give the results summarized in Table 1. In a few cases we find concurrent models of similar fit quality and we give their parameters in the consecutive rows of Table 1. In the third column of the table we assess the character of the events. In 19 cases (of 25 investigated) the events are safe binary lens phenomena in our opinion (designated "b" in Table 1). There are three cases classified as double source events ("d" in Table 1) and three events with low quality fits ("?" in Table 1). The source paths and model light curves are shown in the first part of Appendix.

The results of double source modeling are summarized in Table 2. The double source modeling is applied to the majority of the binary lens candidates and some other non-standard events. While formally the fits are usually better for binary lenses, in a few cases we prefer double source models as more natural, giving less complicated light curves. The comparison of two kinds of fits is given in the second part of Appendix, and the well separated double source events – in the third.

Our sample of binary lenses includes now $10+15+19=44$ events of Paper I, Paper II, and the present work, some of them with multiple models. Using the sample we study the distributions of various binary lens parameters. In Fig. 1 we show the histograms for the mass ratio and the binary separation. The mass ratio is practically limited to the range $0.1 \leq q \leq 1$ with very small probability of finding a model in the range $0.01 \rightarrow 0.1$ and a single planetary lens with $q < 0.01$.

T a b l e 2

Parameters of double source modeling

| Year | Event | $\chi^2$/DOF | $b_1$ | $b_2$ | $t_{01}$ | $t_{02}$ | $t_{\rm E}$ | $f_1$ | $f_2$ |
|---|---|---|---|---|---|---|---|---|---|
| 2004 | 004 | 1054./849 | 0.8803 | 0.0014 | 3048.75 | 3063.12 | 12.1 | 0.996 | 0.004 |
| 2004 | 226 | 404./312 | 0.0591 | 0.0067 | 3137.71 | 3148.21 | 71.1 | 0.109 | 0.014 |
| 2004 | 280 | 597./242 | 0.0684 | 0.0057 | 3167.15 | 3186.43 | 122.6 | 0.021 | 0.008 |
| 2004 | 328 | 244./277 | 0.7078 | 0.0080 | 3177.45 | 3255.48 | 12.9 | 0.935 | 0.065 |
| 2004 | 347 | 368./294 | 0.1749 | 0.0790 | 3204.96 | 3219.74 | 45.9 | 0.276 | 0.140 |
| 2004 | 354 | 1857./338 | 0.7987 | 0.4766 | 3176.11 | 3192.13 | 3.5 | 0.865 | 0.135 |
| 2004 | 362 | 746./419 | 0.0000 | 0.0259 | 3200.43 | 3210.20 | 483.3 | 0.000 | 0.005 |
| 2004 | 366 | 650./221 | 1.1336 | 0.0125 | 3169.15 | 3180.90 | 10.1 | 0.979 | 0.021 |
| 2004 | 367 | 2480./298 | 0.0151 | 0.0124 | 3179.86 | 3181.00 | 20.1 | 0.108 | 0.461 |
| 2004 | 406 | 546./408 | 0.1870 | 0.0000 | 3190.99 | 3195.64 | 8.8 | 1.000 | 0.000 |
| 2004 | 444 | 255./243 | 2.0329 | 0.0001 | 3190.11 | 3204.32 | 8.1 | 0.993 | 0.007 |
| 2004 | 451 | 405./314 | 0.0976 | 0.0001 | 3205.18 | 3225.93 | 28.1 | 0.079 | 0.007 |
| 2004 | 460 | 375./346 | 0.7770 | 0.0000 | 3199.70 | 3210.71 | 19.4 | 1.000 | 0.000 |
| 2004 | 480 | 501./343 | 0.0001 | 0.2528 | 3219.32 | 3225.11 | 10.5 | 0.099 | 0.901 |
| 2004 | 490 | 291./316 | 0.1745 | 0.0004 | 3222.93 | 3238.96 | 17.7 | 0.373 | 0.009 |
| 2004 | 559 | 3489./202 | 0.1343 | 0.1559 | 3258.82 | 3266.48 | 10.2 | 0.699 | 0.301 |
| 2004 | 572 | 399./243 | 0.1962 | 0.3326 | 3275.19 | 3301.65 | 27.6 | 0.374 | 0.626 |
| 2004 | 605 | 380./413 | 0.0002 | 0.0007 | 3297.45 | 3316.19 | 42.5 | 0.245 | 0.210 |

Note: The columns contain: the year and event number according to EWS, the rescaled $\chi^2$ value and the DOF number, the impact parameters $b_1$ and $b_2$ for the two source components, times of the closest approaches $t_{01}$ and $t_{02}$, the Einstein time $t_{\rm E}$, and the blending parameters $f_1 = F_{s1}/(F_{s1}+F_{s2}+F_b)$ and $f_2 = F_{s2}/(F_{s1}+F_{s2}+F_b)$.

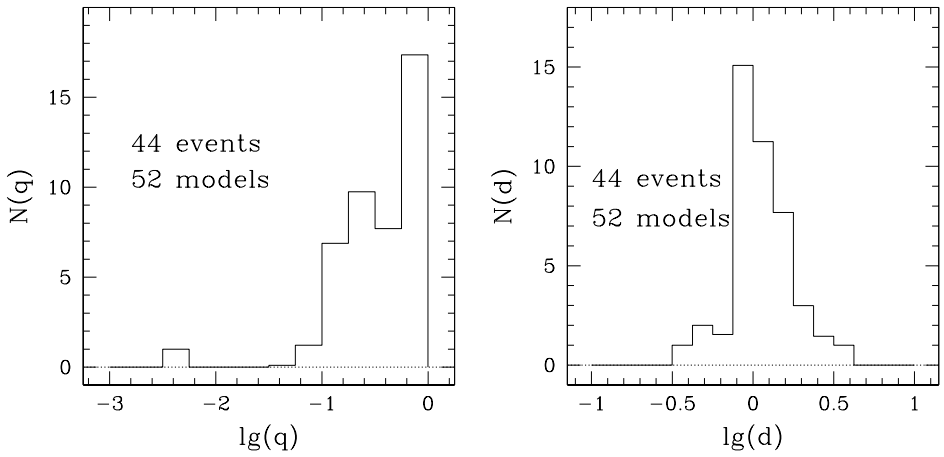


Fig. 1. Histogram of mass ratios (*left*) and separations (*right*) for binary lens events of OGLE-II (Paper I) and OGLE-III (Paper II and this work). The histogram includes 44 events, some of them with multiple models. The alternative models of any event have been assigned fractional weights.

## 5. Discussion

Our classification of the investigated events into the binary lens double source/ unknown categories needs further explanation. The binary lens model of the event 367 is rather superficial with its four maxima in the light curve, while there is only one in the data; the double source model is more natural, but we reject it on the basis of low fit quality. Both kinds of models for the event 444 are formally acceptable, but not compelling because of the low flux amplitude. In the case of 559, the binary lens model looks superficial (case similar to 367) and the double source model gives a very poor fit. We include event 347 in the double source category despite the better formal quality of the binary lens fit. We choose the binary lens interpretation for the event 280, since its light curve exhibits three maxima (two of them rather weak) and the double source model is qualitatively wrong. For the events 490 and 605 we choose the double source interpretation because such models are simpler as compared to binary lens models, with formally similar quality. In the case of 226 we arbitrarily choose binary lens interpretation, despite the existence of the similar quality double source model.

Our sample of OGLE binary lens events contains now 44 cases. The bimodality of the mass ratio distribution and the lack of intermediate $q$ values remains a valid interpretation of the data. We are not trying a statistical interpretation of mass ratio distribution in this paper skipping it into a future publication including events of 2005 season with another three planetary lenses.

We neglect parallax effect in the binary lens models included in this work. The inclusion of the effect improves some of the presented models, but the difference is never dramatic. Since simultaneous measurement of the parallax effect and the source size allows the lens mass estimation (An *et al.* 2002) we are going to investigate it with detail in a paper devoted to events with observations covering caustic crossings.

**Acknowledgements.** We thank Bohdan Paczyński for many helpful discussions and Shude Mao for the permission of using his binary lens modeling software. This work was supported in part by the Polish MNiSW grant 2-P03D-016-24, the NSF grant AST-0607070, and NASA grant NNG06GE27G.

## REFERENCES

Alard, C. 2000, *Astron. Astrophys. Suppl. Ser.*, **144**, 363.
Alard, C., and Lupton, R.H. 1998, *Astrophys. J.*, **503**, 325.
Albrow, M.D., *et al.* 1999, *Astrophys. J.*, **522**, 1022.
Alcock, C., *et al.* 2000, *Astrophys. J.*, **541**, 270.
An, J.H., *et al.* 2002, *Astrophys. J.*, **572**, 521.
Beaulieu, J.-P., *et al.* 2006, *Nature*, **439**, 437.
Bond, I.A., *et al.* 2004, *Astrophys. J. Letters*, **606**, L155.
DiStefano, R., and Mao, S. 1996, *Astrophys. J.*, **457**, 93.

Dominik, M. 1998, *Astron. Astrophys.*, **333**, L79.
Gaudi, B.S., and Han, Ch. 2004, *Astrophys. J.*, **611**, 528.
Gould, A., *et al.* 2006, *Astrophys. J. Letters*, **644**, L37.
Jaroszyński, M. 2002, *Acta Astron.*, **52**, 39 (Paper I).
Jaroszyński, M., Udalski, A., Kubiak, M., Szymański, M., Pietrzyński, G., Soszyński, I., Żebruń, K., Szewczyk, O., and Wyrzykowski, Ł. 2004, *Acta Astron.*, **54**, 103 (Paper II).
Mao, S., and DiStefano, R. 1995, *Astrophys. J.*, **440**, 22.
Mao, S., and Loeb, A. 2001, *Astrophys. J. Letters*, **547**, L97.
Mao, S., and Paczyński, B. 1991, *Astrophys. J. Letters*, **374**, L37.
Paczyński, B. 1996, *Ann. Rev. Astron. Astrophys.*, **34**, 419, "Gravitational Lenses", Springer, Berlin.
Schneider, P., and Weiss, A. 1986, *Astron. Astrophys.*, **164**, 237.
Udalski, A. 2003, *Acta Astron.*, **53**, 291.
Udalski, A., *et al.* 2005, *Astrophys. J. Letters*, **628**, L109.
Udalski, A., Szymański, M., Kaluzny, J., Kubiak, M., Mateo, M., Krzemiński, W., and Paczyński, B. 1994, *Acta Astron.*, **44**, 227.
Wyrzykowski, Ł. 2005, PhD Thesis, Warsaw University Astronomical Observatory.

## Appendix

*Binary Lens Models*

Below we present plots for the 25 events for which the binary lens modeling has been applied. Some of the events, especially cases of heavily blended sources or events without apparent caustic crossing, may have alternative double source models. In such cases we show the comparison of the binary lens and double source fits to the data in the next subsection.

The events are ordered and named according to their position in the OGLE EWS database for the season 2004. Some events have more than one binary lens model of comparable fit quality (compare Table 1). We always show the best (first) model, and the second one only if it is not rejected at 95% confidence level based on the difference in its $\chi^2$ value.

Each case is illustrated with two panels. The most interesting part of the source trajectory, the binary and its caustic structure are shown in the left panel for the case considered. The labels give the $q$ and $d$ values. On the right panels the part of the best fit light curve is compared with observations. The labels give the rescaled $\chi^2_1$ /DOF values. The source radius (as projected into the lens plane and expressed in Einstein radius units) is labeled only for three events with resolved caustic crossings. Below the light curves we show the differences between the observed and modeled flux in units of rescaled errors. The dotted lines show the $\pm 3\sigma$ band.

**OGLE 2004-BLG-035**

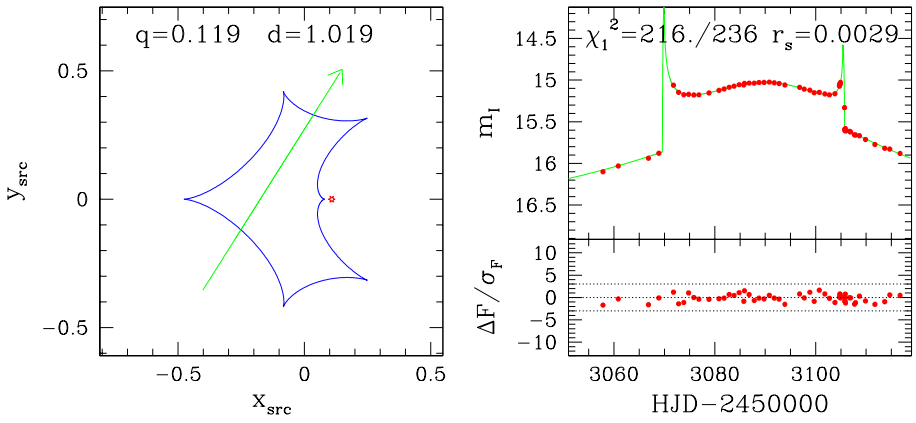

**OGLE 2004-BLG-039**

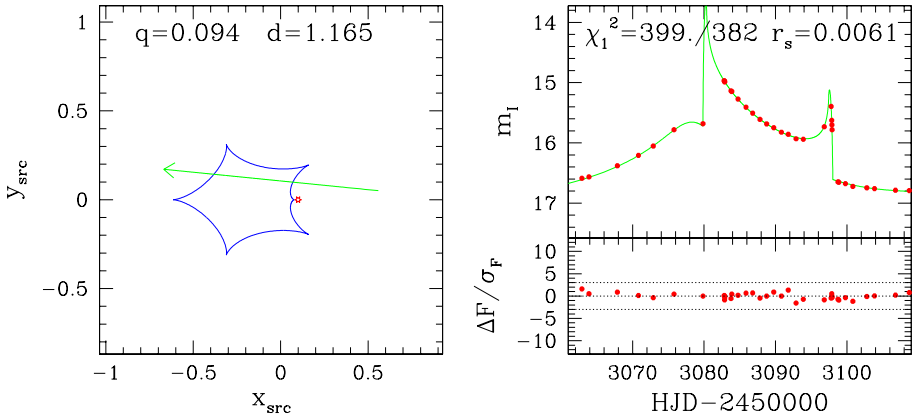


**OGLE 2004-BLG-207**

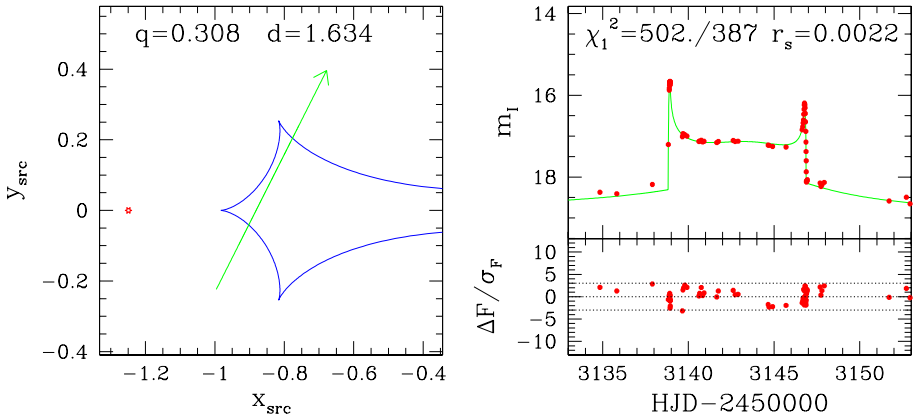


**OGLE 2004-BLG-226: I**

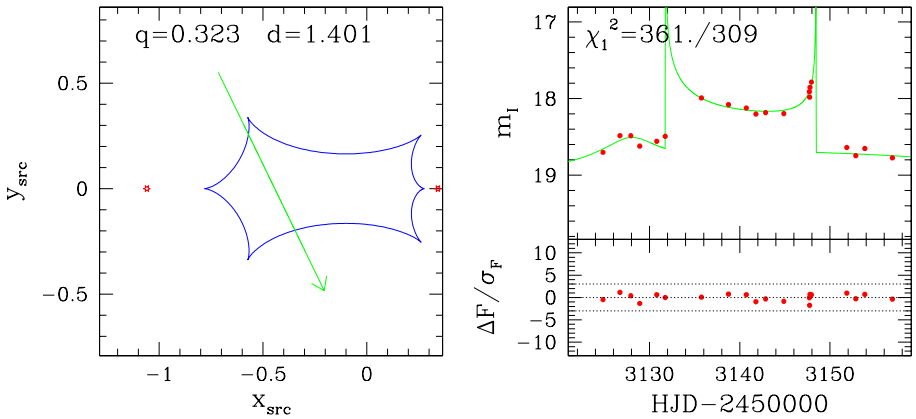

**OGLE 2004-BLG-226: II**

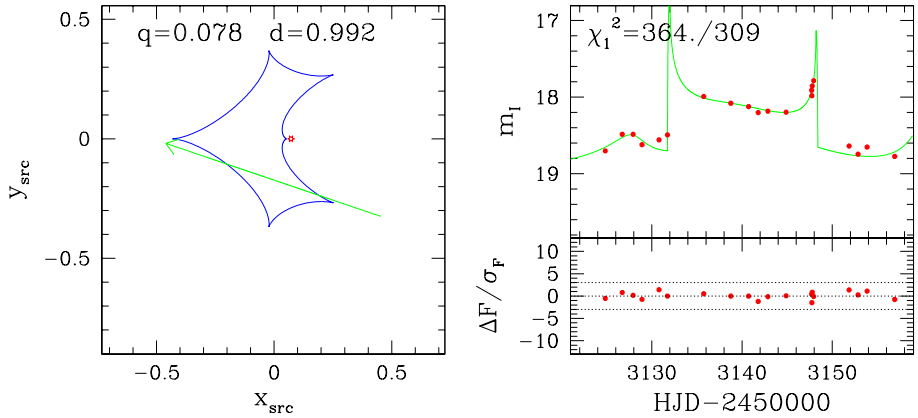


**OGLE 2004-BLG-250**

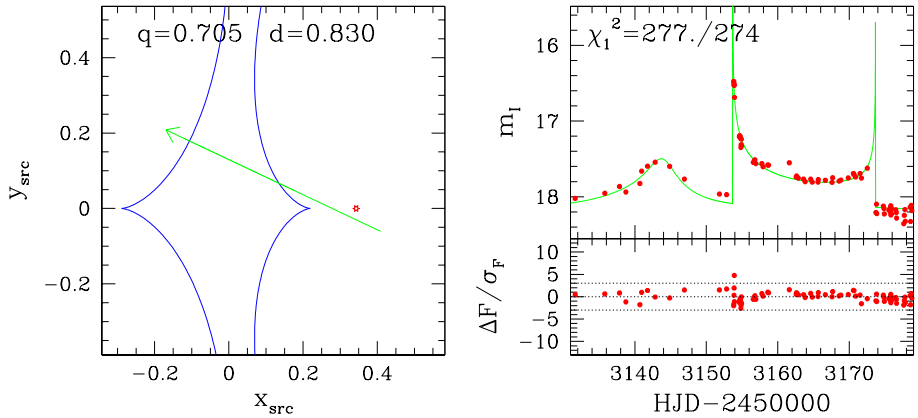


**OGLE 2004-BLG-273**

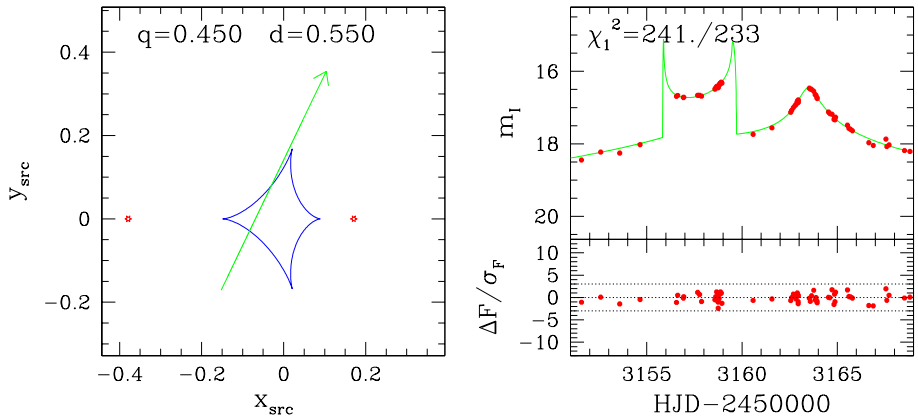

**OGLE 2004-BLG-280**

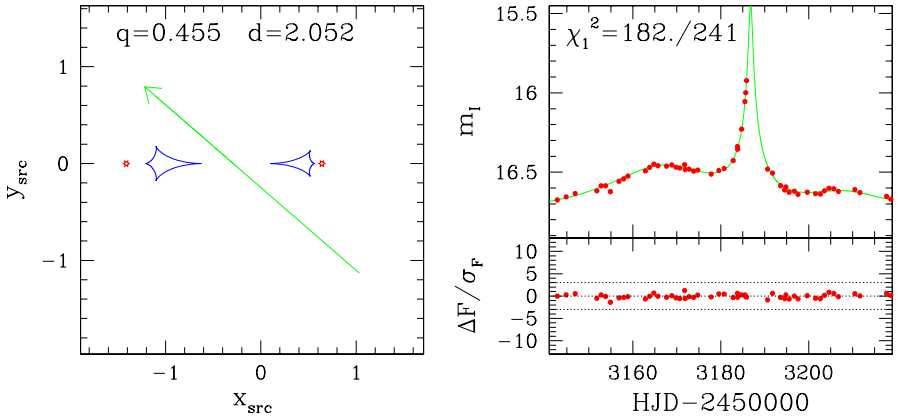


**OGLE 2004-BLG-309**

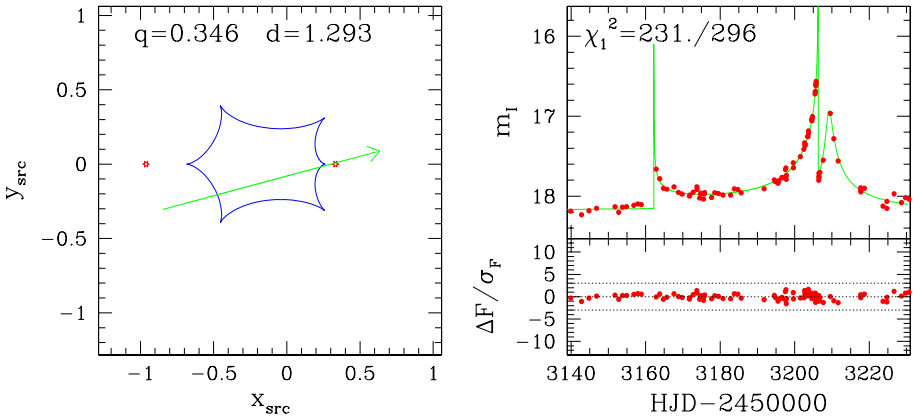


**OGLE 2004-BLG-325**

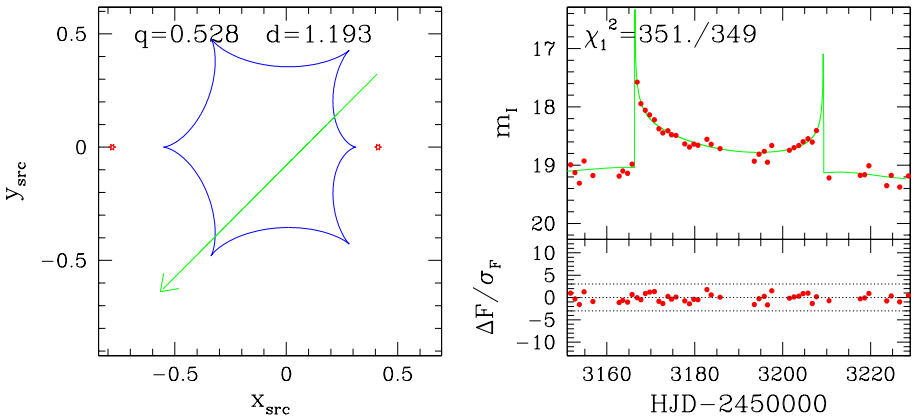

**OGLE 2004-BLG-347: I**

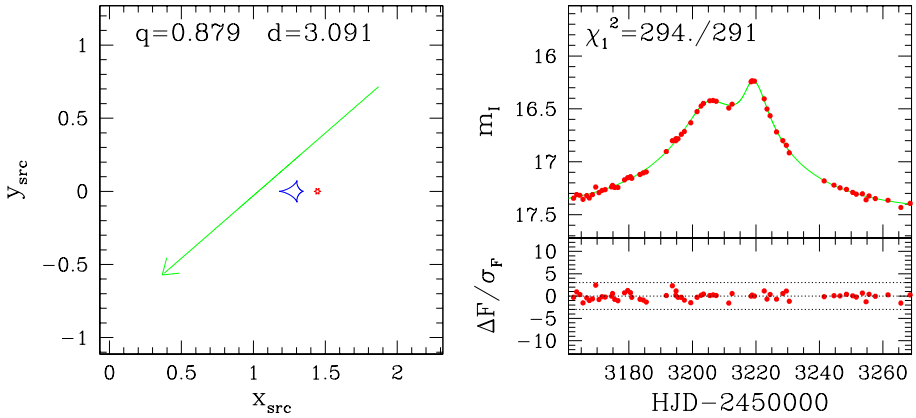


**OGLE 2004-BLG-347: II**

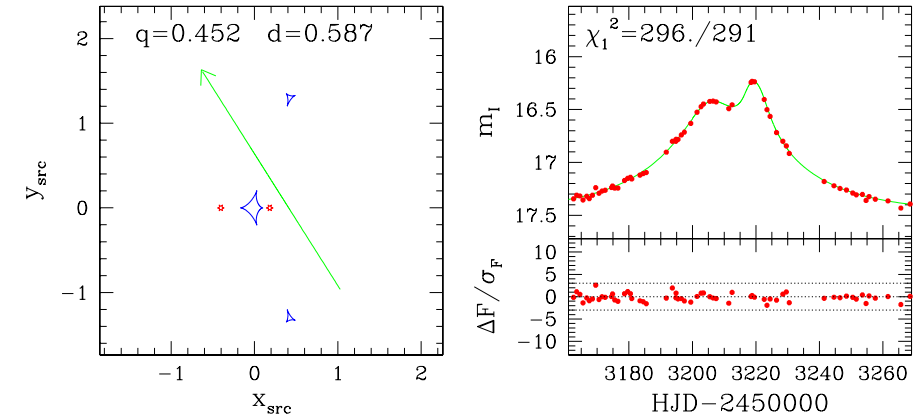


**OGLE 2004-BLG-354**

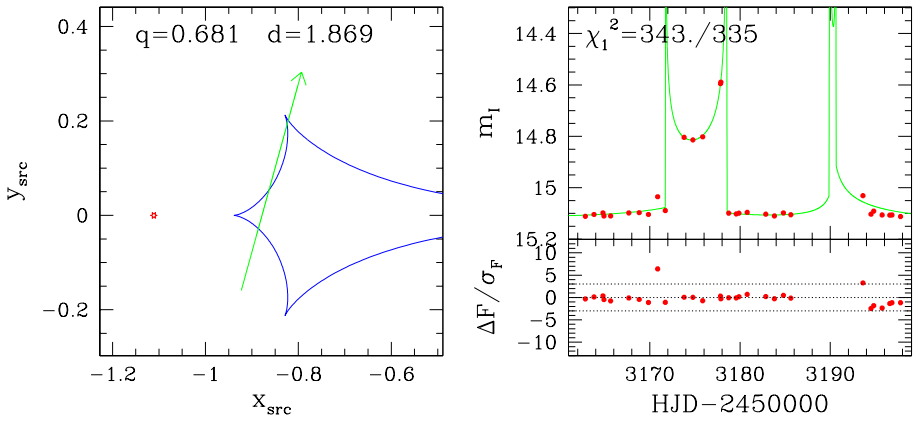

**OGLE 2004-BLG-362**

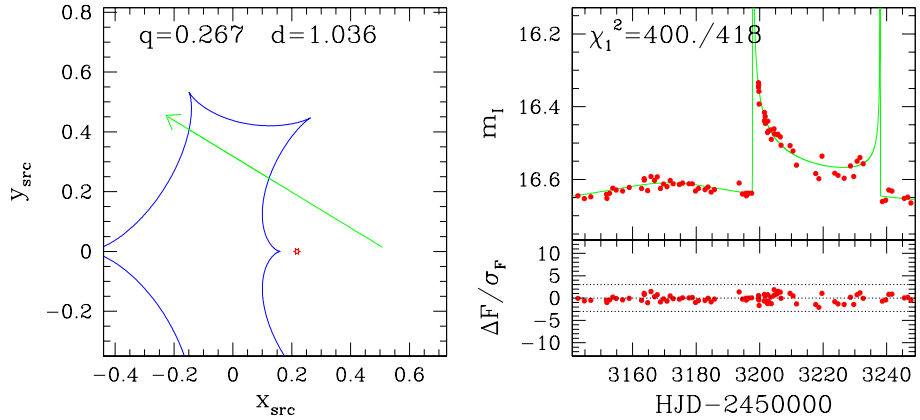


**OGLE 2004-BLG-366**

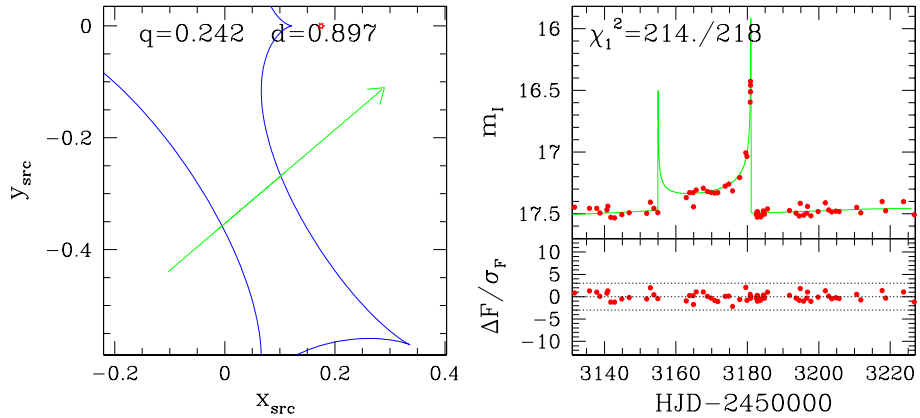


**OGLE 2004-BLG-367**

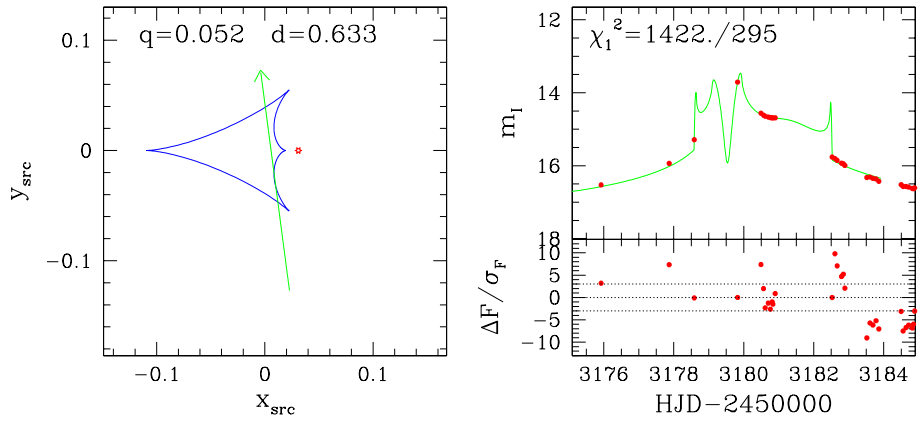

**OGLE 2004-BLG-373**

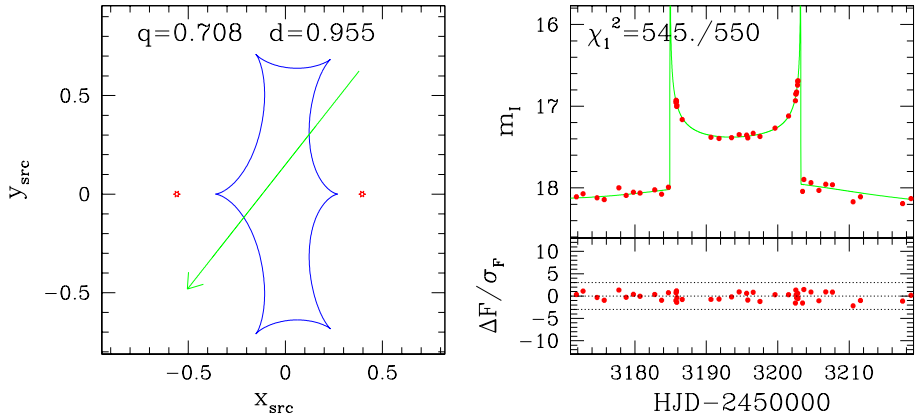


**OGLE 2004-BLG-379**

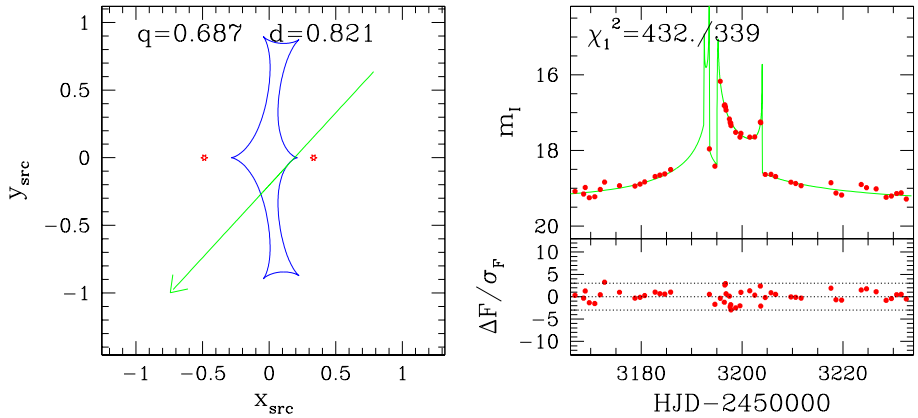


**OGLE 2004-BLG-406: I**

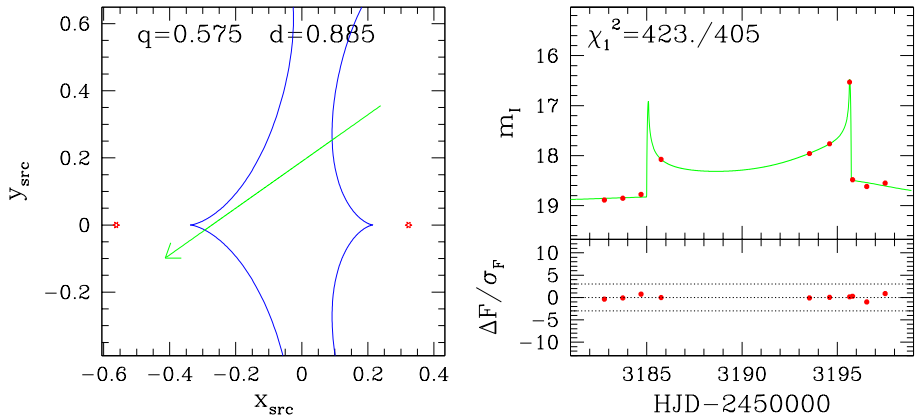

**OGLE 2004-BLG-406: II**

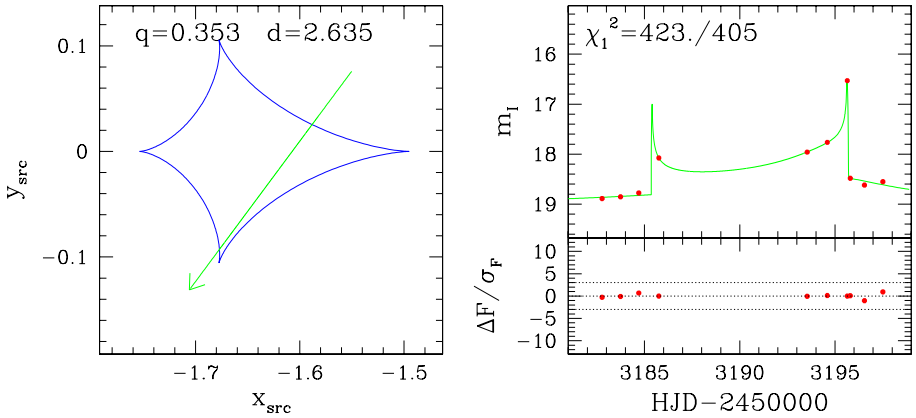


**OGLE 2004-BLG-444**

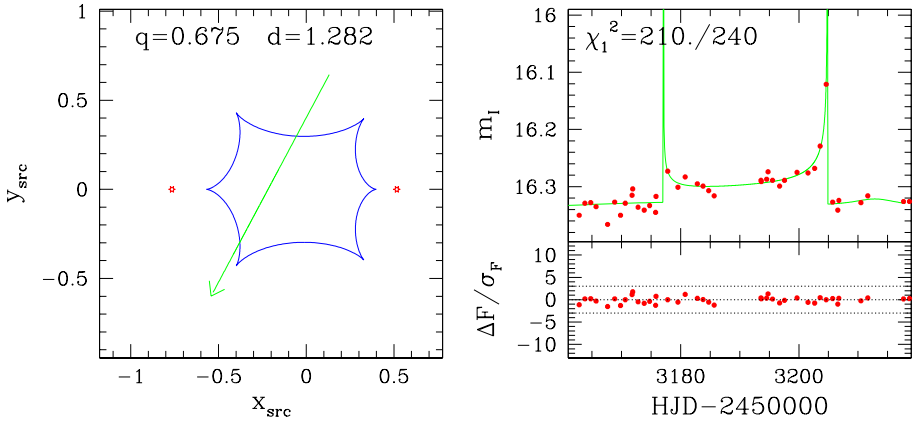


**OGLE 2004-BLG-451**

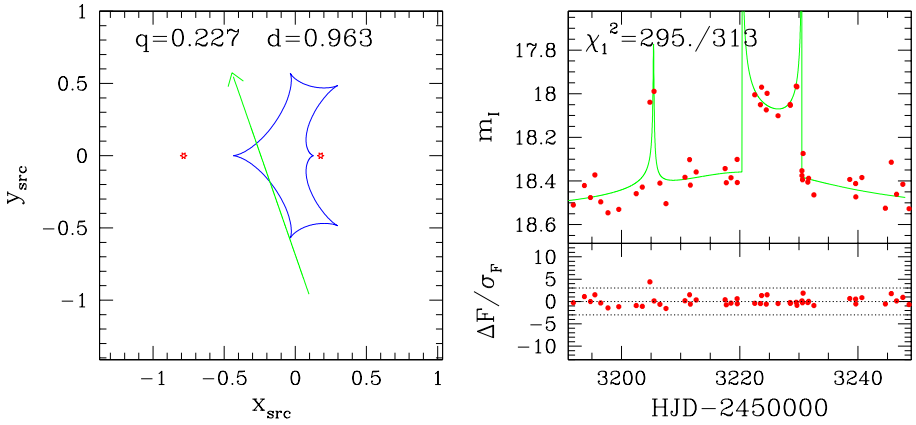

**OGLE 2004-BLG-460: I**

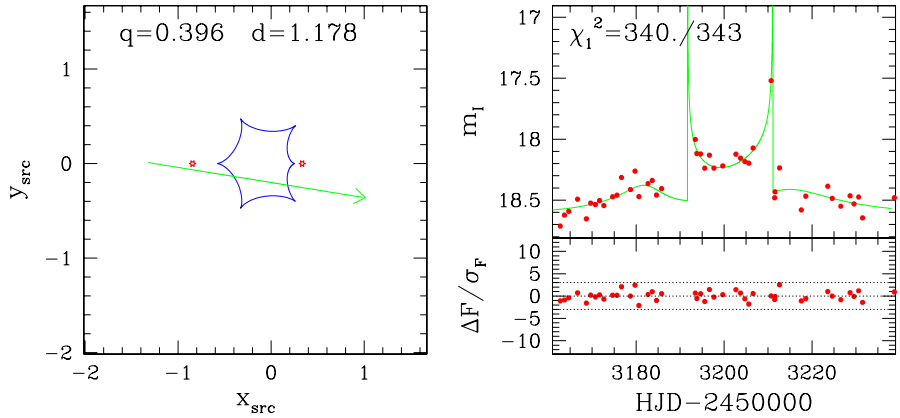


**OGLE 2004-BLG-460: II**

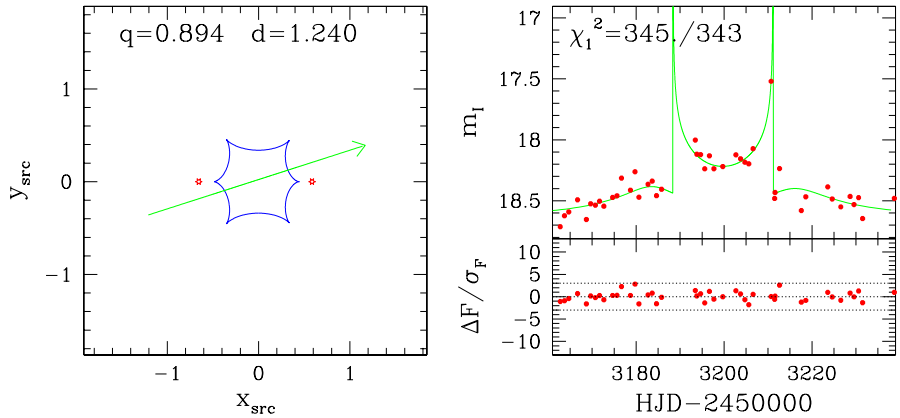


**OGLE 2004-BLG-480: I**

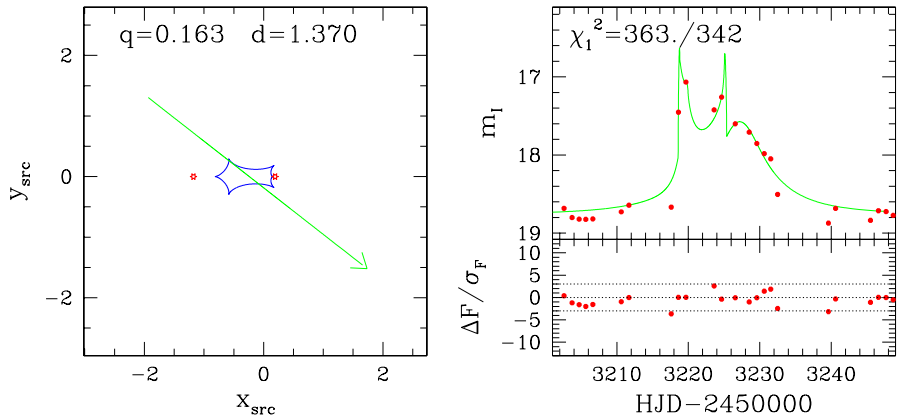

**OGLE 2004-BLG-480: II**

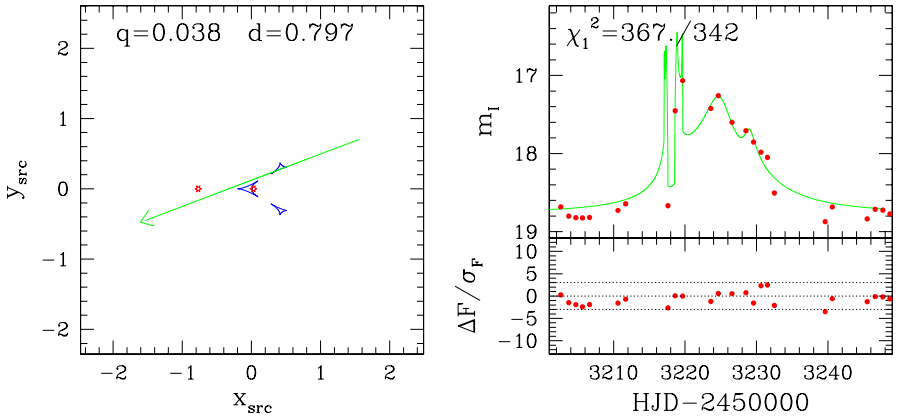


**OGLE 2004-BLG-490: I**

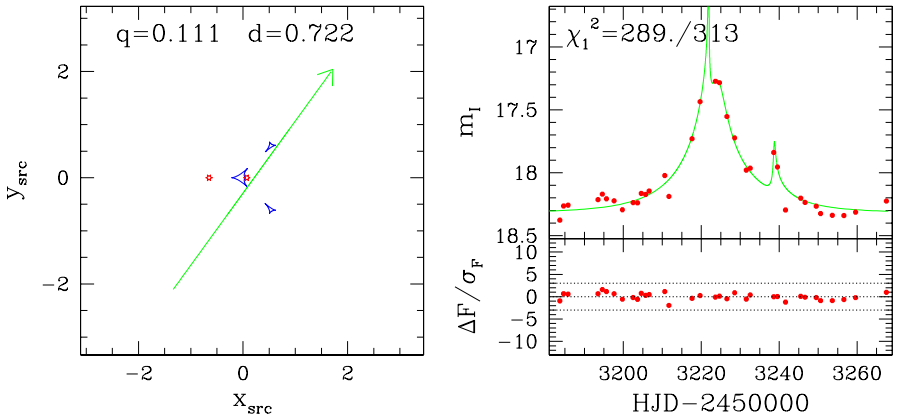


**OGLE 2004-BLG-490: II**

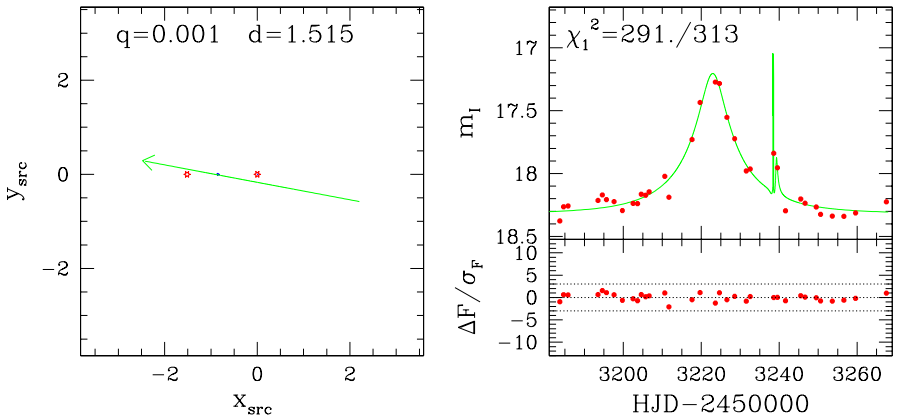

**OGLE 2004-BLG-559**

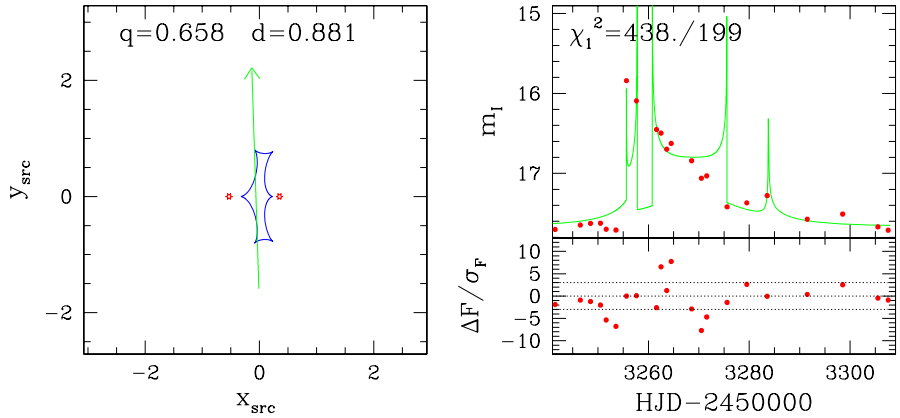


**OGLE 2004-BLG-572**

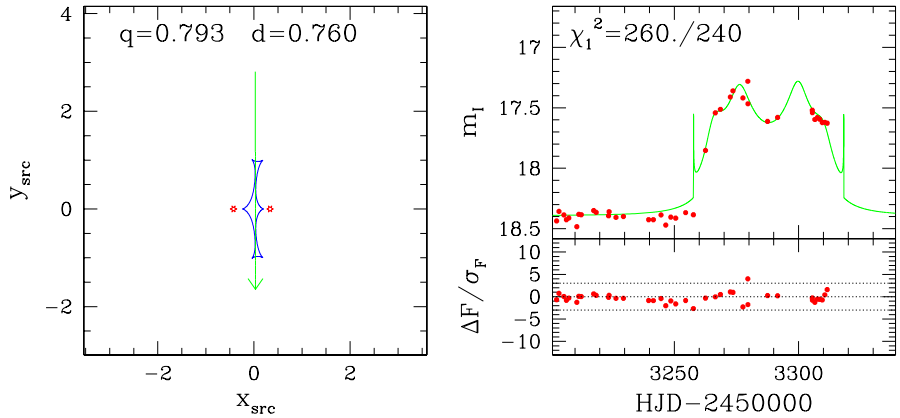


**OGLE 2004-BLG-605: I**

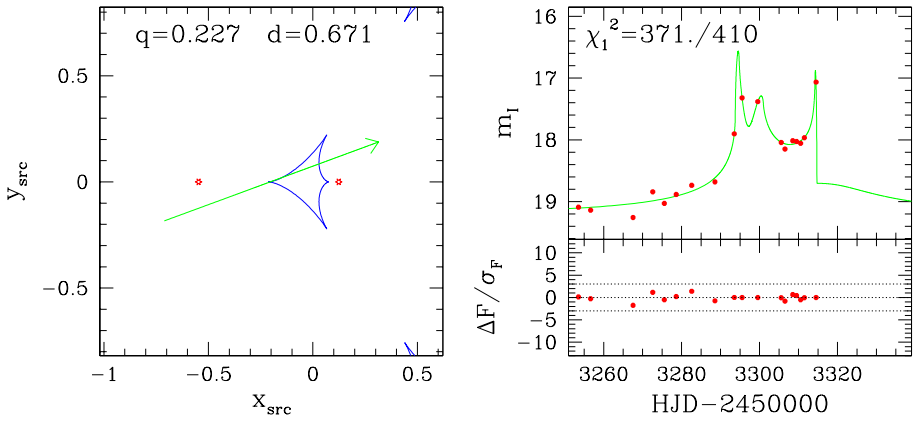

**OGLE 2004-BLG-605: II**

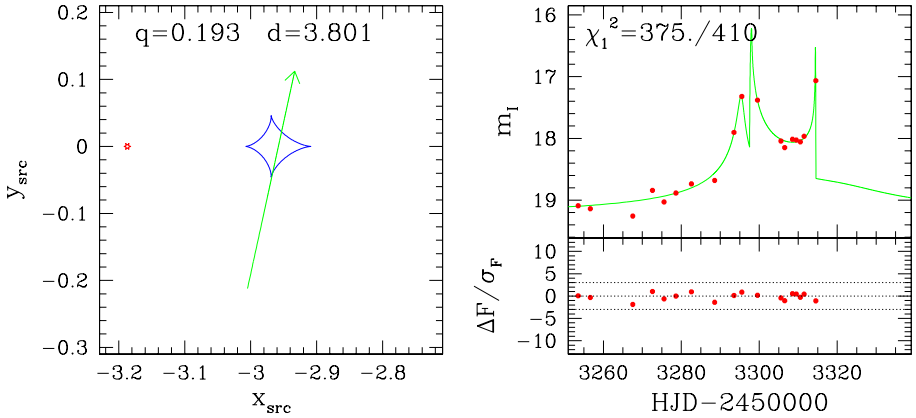


*Ambiguous Binary Lens/Double Source Events*

Below we show the binary lens (on the left) and double source (on the right) models of the light curves for some of the considered events. The light curve in a double source model is a sum of the constant blended flux plus the two single lens light curves for the source components, each shown with dotted lines. We use fluxes for both kind of models to ensure a better comparison. In majority of cases the binary lens models give formally better fits as compared to the double source models presented. On the other hand double source models, always producing simpler light curves, look more natural in some cases.

**OGLE 2004-BLG-226**

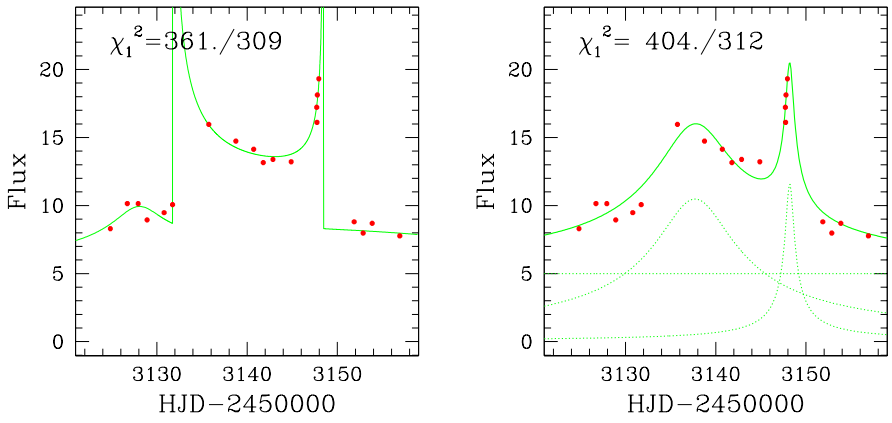

**OGLE 2004-BLG-280**

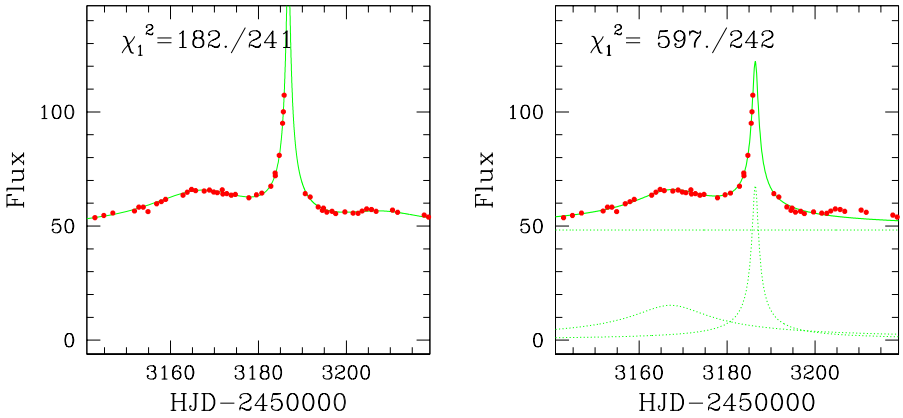


**OGLE 2004-BLG-347**

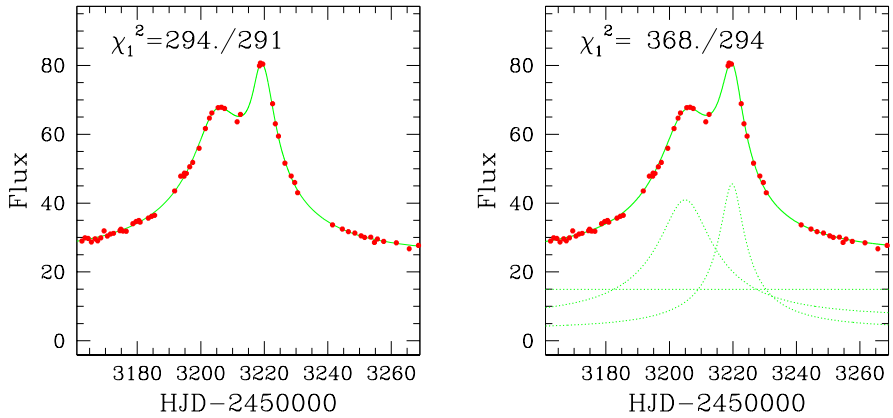


**OGLE 2004-BLG-354**

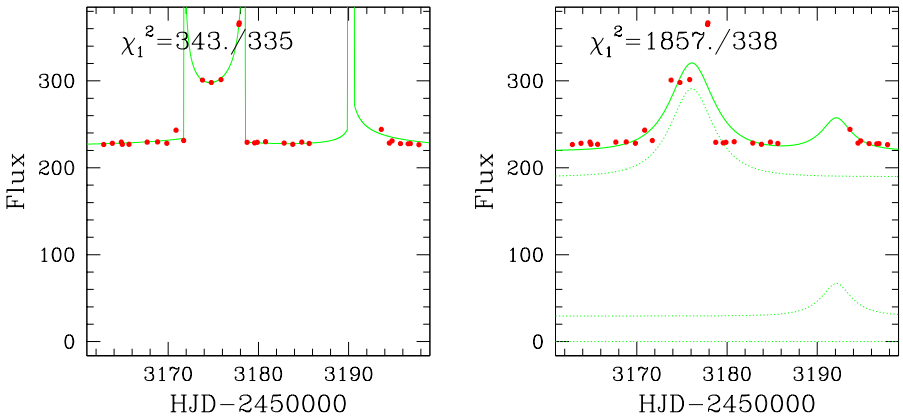

**OGLE 2004-BLG-362**

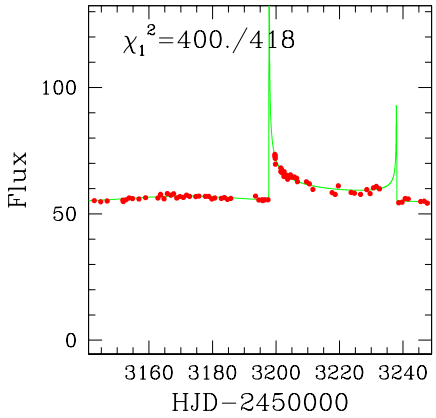


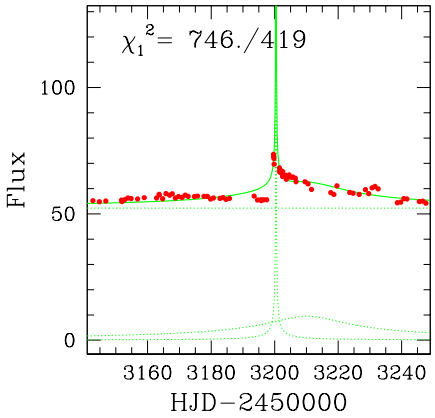


**OGLE 2004-BLG-366**

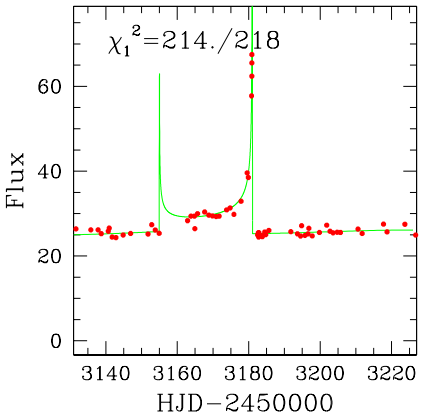


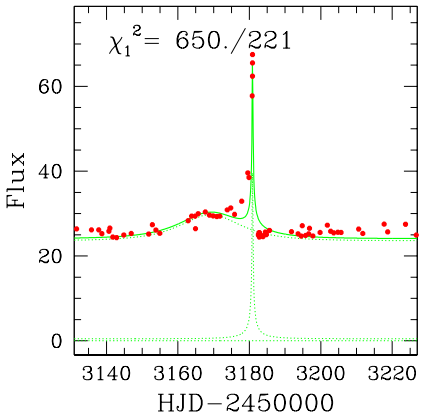


**OGLE 2004-BLG-367**

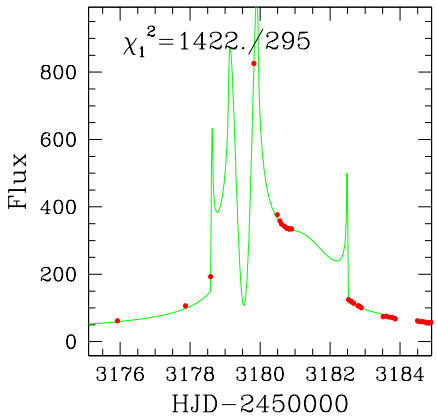


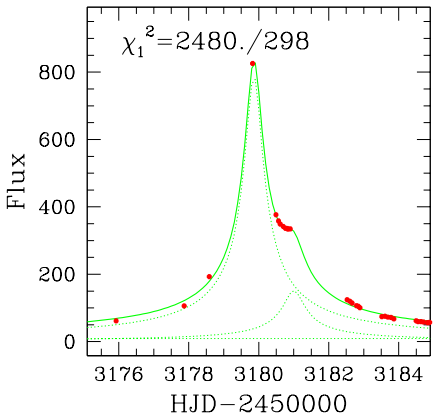

**OGLE 2004-BLG-444**

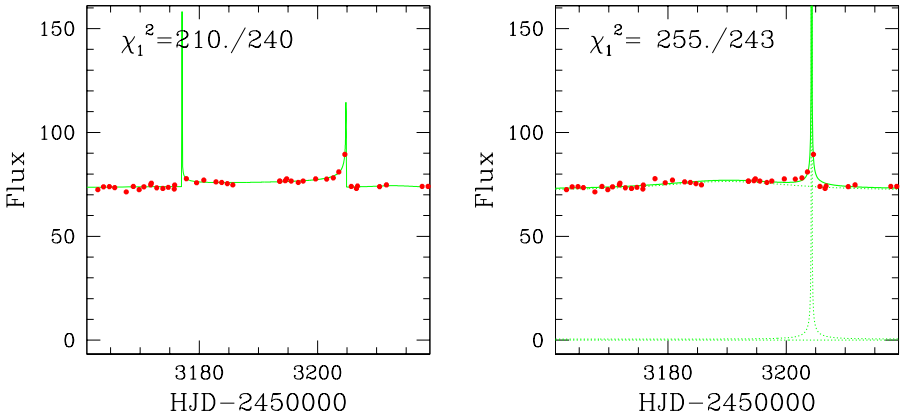


**OGLE 2004-BLG-451**

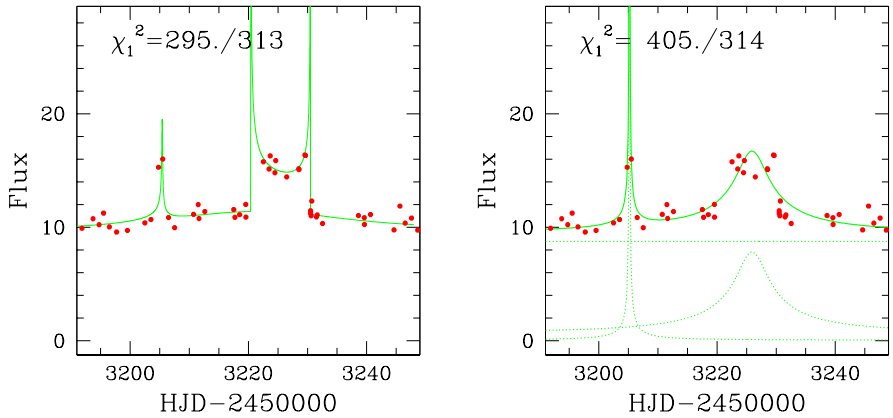


**OGLE 2004-BLG-460**

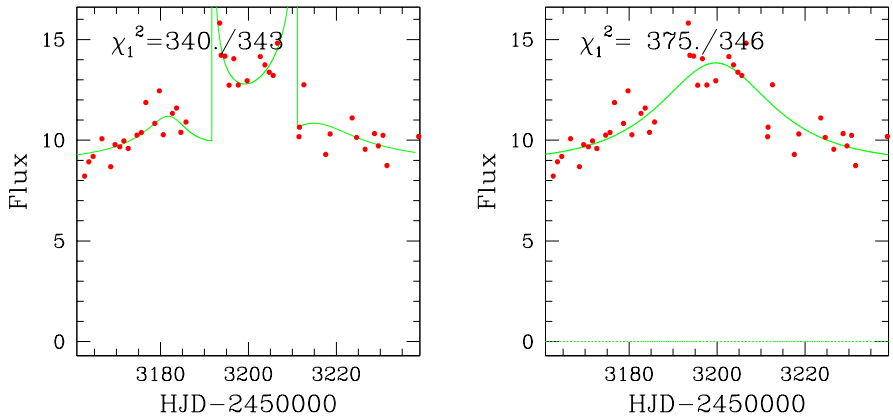

**OGLE 2004-BLG-480**

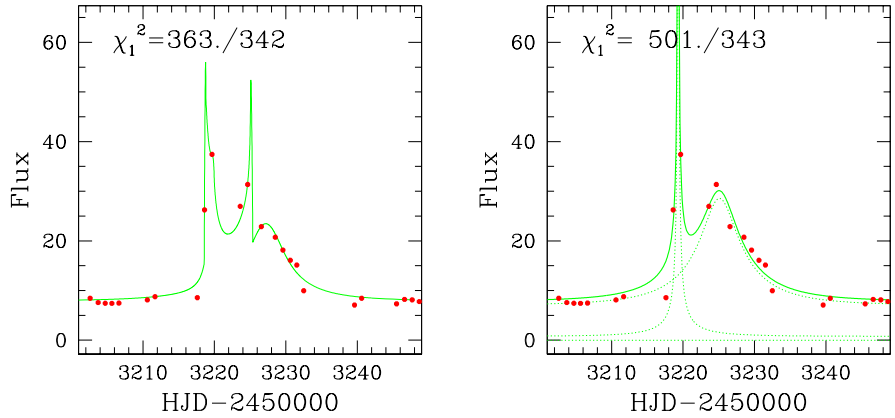


**OGLE 2004-BLG-490**

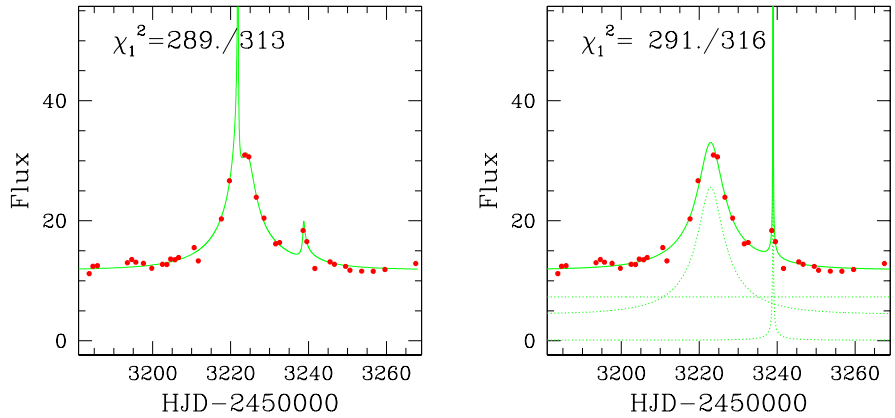


**OGLE 2004-BLG-559**

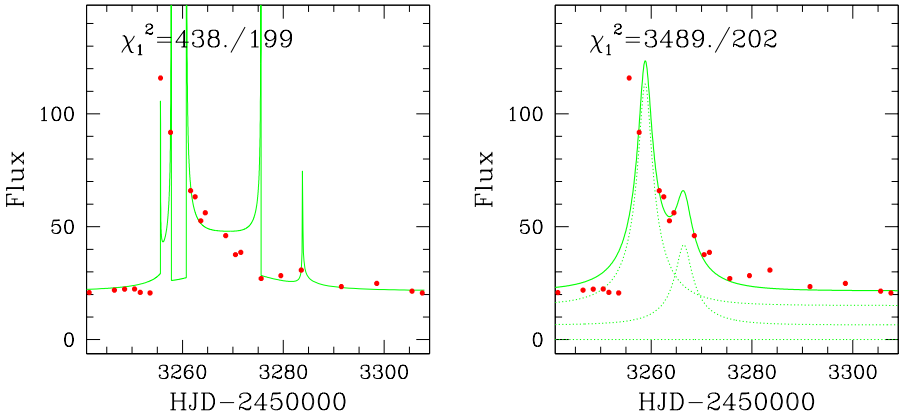

**OGLE 2004-BLG-572**

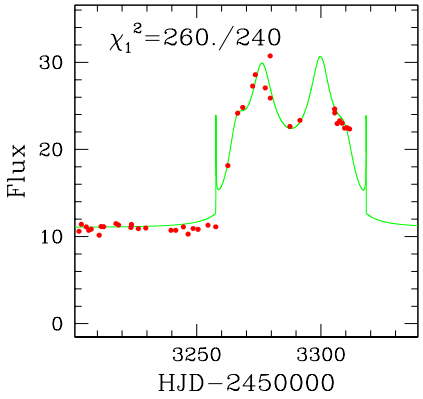


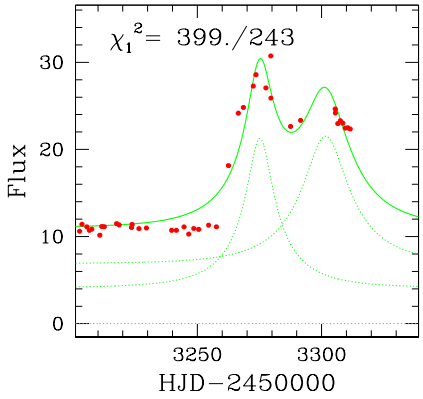


**OGLE 2004-BLG-605**

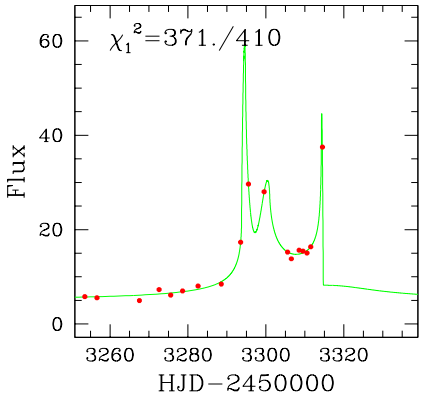


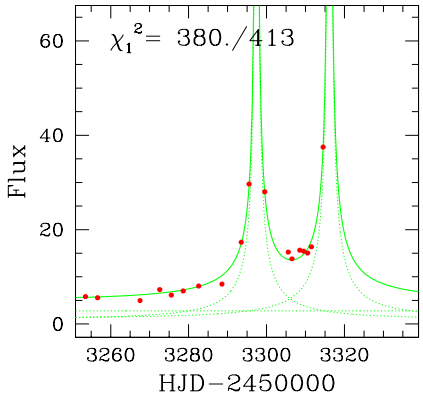


*Double source events*

**OGLE 2004-BLG-004**

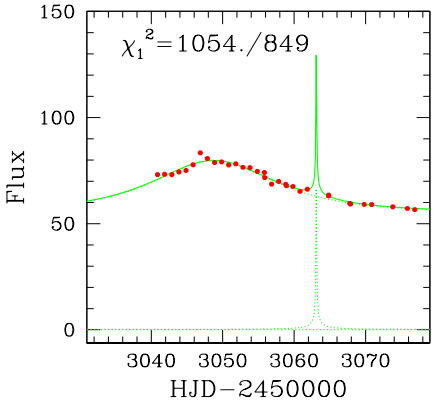


**OGLE 2004-BLG-328**